A comparative study of cave system Ca isotope ratios with rainfall, δ13C, and trace element data: Implications for quantitative reconstructions of paleorainfall from speleothems

This presentation participates in OSPP

EGU

Outstanding Student & PhD candidate Presentation contest

Cameron de Wet[1]*, Elizabeth Griffith[2], Andrea Erhardt[3], Harold Bradbury[4], Alexandra Turchyn[4], Jessica Oster[1]

[1]Vanderbilt University; [2]The Ohio State University; [3]University of Kentucky; [4]University of Cambridge

*Cameron.de.wet@vanderbilt.edu

THE GEOLOGICAL SOCIETY OF AMERICA®

KARST WATERS INSTITUTE

CRF

NATIONAL SPELEOLOGICAL SOCIETY

VANDERBILT UNIVERSITY

Introduction

- Speleothem Ca ratios (δ^{44}Ca) are thought to be uniquely controlled by prior calcite precipitation (PCP), which can be modeled as a Rayleigh fractionation process[1,2,3,6]:

$$\text{Eq. 1} \qquad f = \left(\frac{r_s}{\alpha * r_0}\right)^{\frac{1}{\alpha-1}}$$

f = fraction of Ca remaining in solution
$r_s = \delta^{44}Ca_{calcite}/1000 + 1$
$r_0 = \delta^{44}Ca_{drip}^{f=1}/1000 + 1$
$\alpha = \alpha_{calcite/drip\ water}$

- When calibrated with modern data, speleothem δ^{44}Ca shows promise as a semi-quantitve proxy for past effective rainfall rates.[2,4,5]

- However, few rigorous cave monitoring studies have focused specifically on modern Ca isotope cycling in cave systems and the ways in which precipitation seasonality and non-climate factors influence δ^{44}Ca are not well constrained.

- We present a comparative study of δ^{44}Ca data and coeval measurements of δ^{13}C and trace element ratios from cave drip waters, farmed calcite, and host rocks from three different cave systems - White Moon Cave, CA (WMC), Lake Shasta Caverns, CA (LSC), and Blue Springs Cave, TN (BS).

- We aim to test the following questions:

1. How do non-climate factors like epikarst thickness or host rock δ^{44}Ca variability/geology influence δ^{44}Ca values in the cave?
2. How does cave system δ^{44}Ca relate to rainfall amount and seasonality?
3. How does cave system δ^{44}Ca compare with established proxies for water infiltration/PCP, like trace element ratios and δ^{13}C?

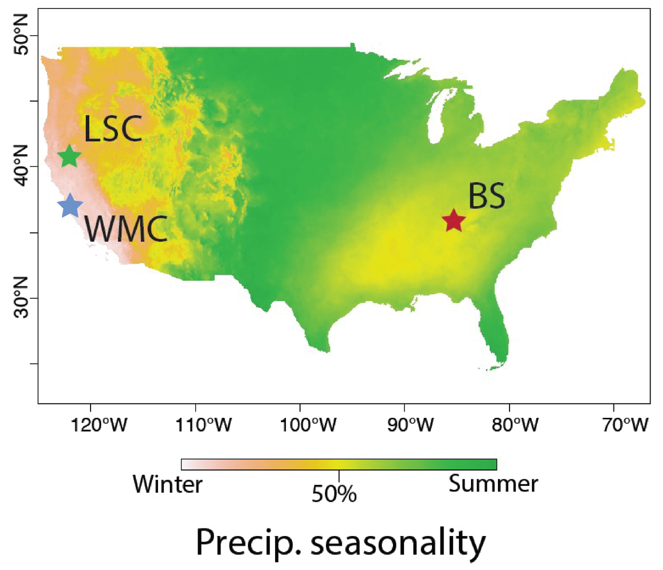

Figure 1. Precipitation seasonality of contiguous US (PRISM 30-year normals).

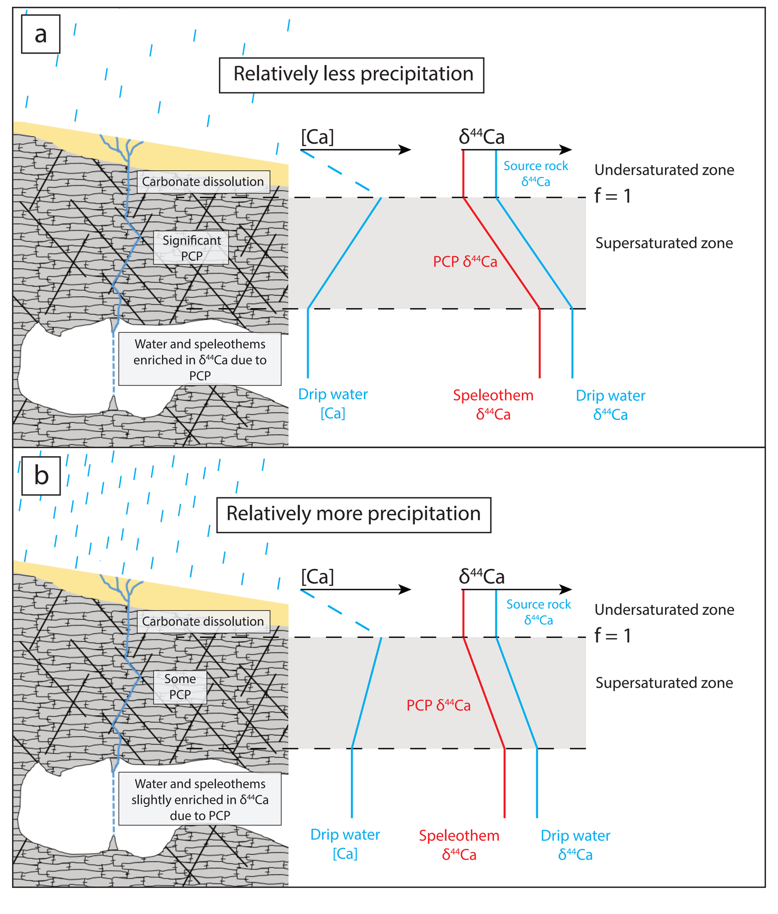

Figure 2. Conceptual model of seepage water flow and [Ca] and δ^{44}Ca evolution under relatively drier (a) and relatively wetter conditions (b). Adapted from Owen et al. (2016).

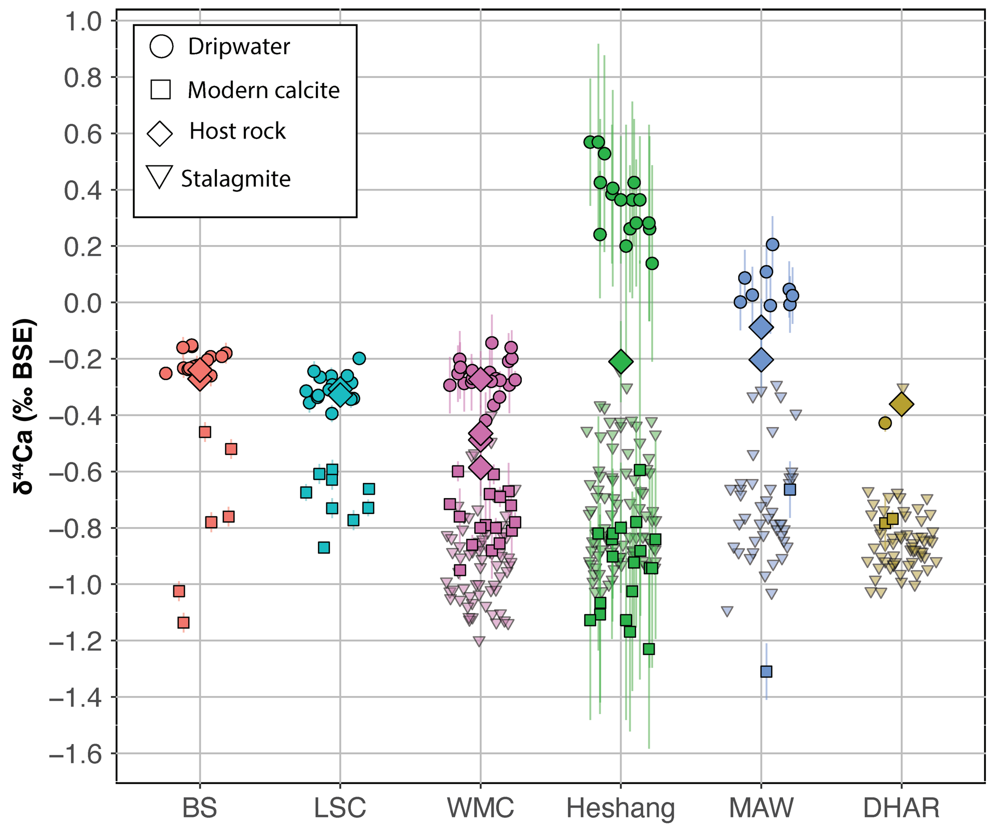

Figure 3. Distribution of drip water, calcite, and carbonate host rock δ44Ca data from Blue Spring Cave (BS), Lake Shasta Caverns (LSC), and White Moon Cave (WMC) (this study, de Wet et al., 2021), Heshang Cave (Owen et al., 2016), Mawmluh Cave (MAW) (Magiera et al., 2019), and Dharamjali Cave (Giesche et al., 2023).

Methods

- WMC δ^{44}Ca samples collected prior to 2.29.20 were analyzed using a ThermoFisher Scientific Triton Plus Thermal Ionization Mass Spectrometer (TIMS) at the Department of Earth Sciences, Cambridge. For these data we report the average external 2σ over the analysis period on NIST 915B (0.1 ‰). BS, LSC, and WMC samples collected post 2.29.20 were analyzed using TIMS at Ohio State University. For these data we report the average external 2σ over the analysis period on NIST 915B (0.04‰).

- BS, LSC, and WMC δ^{13}C were collected using a ThermoFisher Scientific Delta V IRMS equipped with a GasBench at Vanderbilt University. BS, LSC, and WMC trace element ratios were collected using a Thermo Finnigan iCapQ ICP-MS at Vanderbilt University.

- Rainfall data was acquired from the NOAA National Centers for Environmental Information database for stations proximal to the cave sites.

Results

- We present drip water, modern calcite, and host rock δ^{44}Ca measurements from WMC, LSC, and BS at seasonal to annual resolution.

- Drip sites at each cave span a range of depths from the surface and/or drip patterns.

White Moon Cave

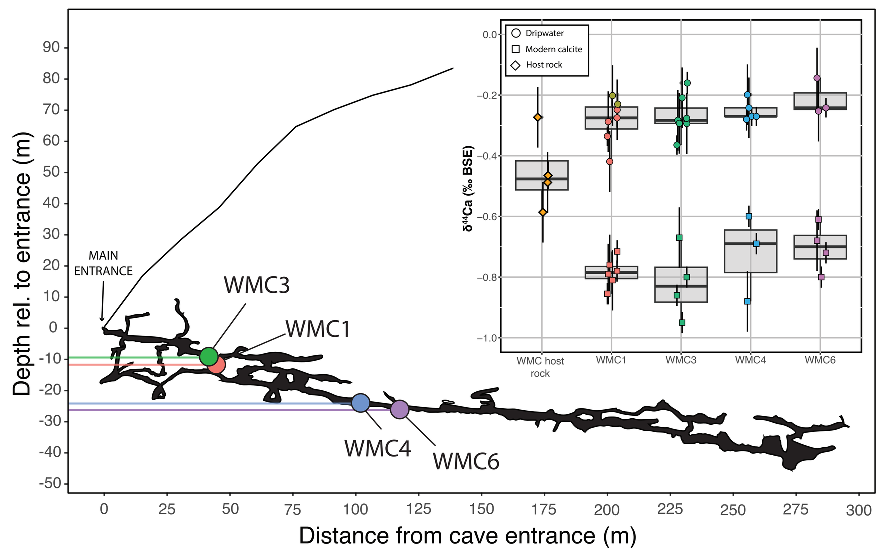

Figure 4. WMC profile with locations and depths of drip sites marked. Inset shows distribution of WMC host rock δ^{44}Ca data and drip water and modern calcite data from each drip monitoring site.

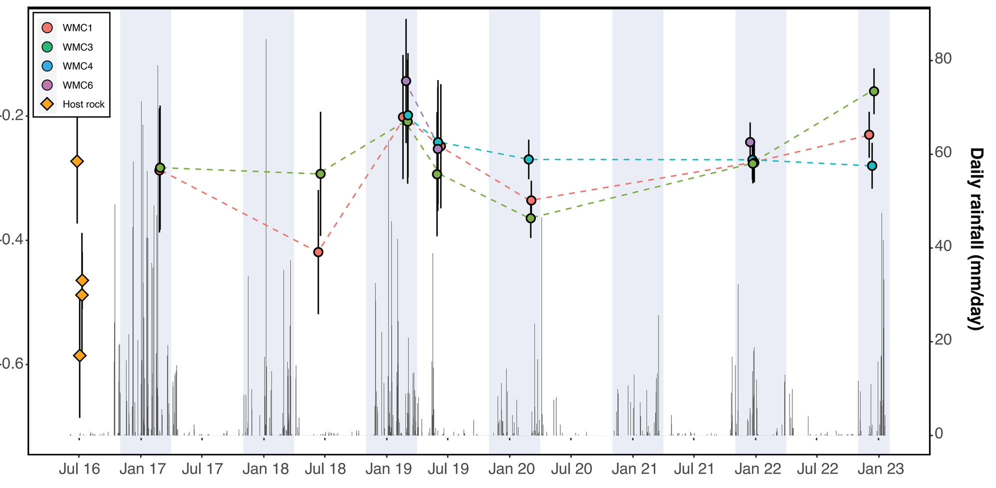

Figure 5. WMC δ^{44}Ca data with daily rainfall amounts from Santa Cruz, CA. Gray bars show cool season (Nov. - April). Points are drip water data. Diamonds are cave host rock measurements.

Lake Shasta Caverns

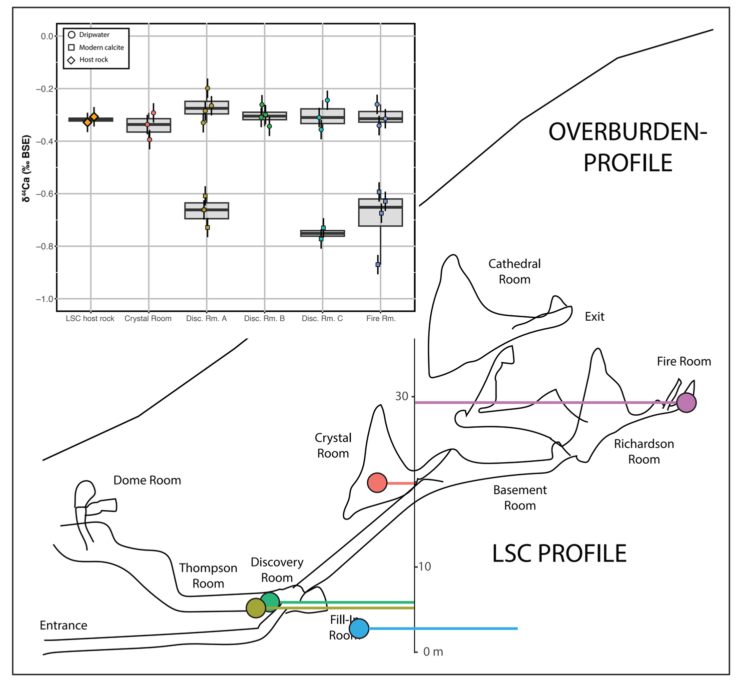

Figure 6. LSC profile with locations and depths of drip sites marked. Inset shows distribution of LSC host rock δ^{44}Ca data and drip water and modern calcite data from each drip monitoring site.

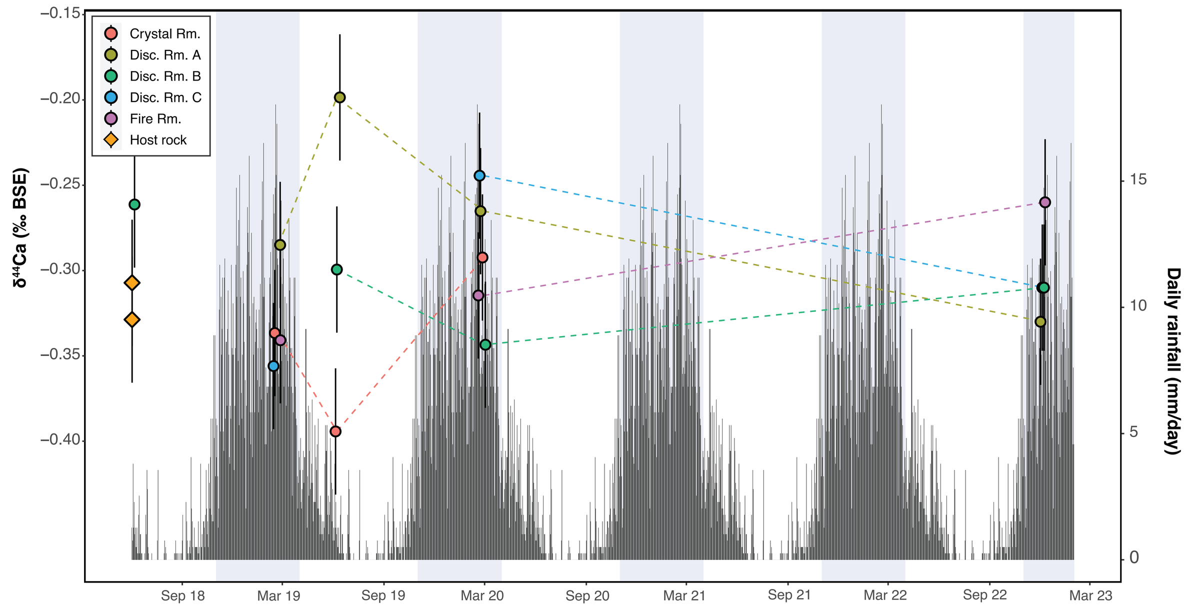

Figure 7. LSC drip water δ^{44}Ca data with daily rainfall amounts from Redding, CA. Gray bars and symbols same as Fig. 5.

Blue Springs Cave

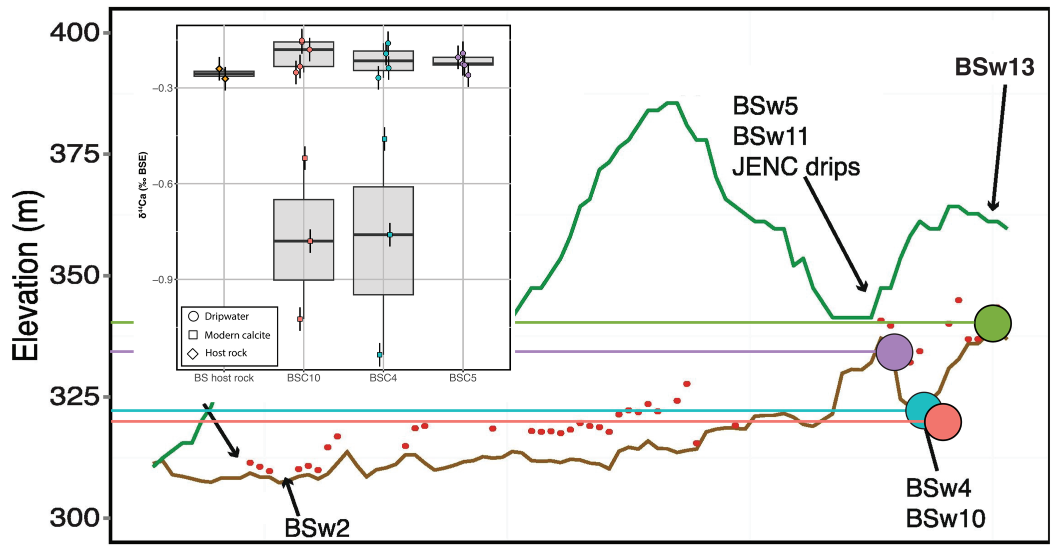

Figure 8. BS profile. Inset shows distribution of LSC host rock δ^{44}Ca data and drip water and modern calcite data from each drip monitoring site. Drip sites BSw5 and BSw13 is fed by fracture flow and sites BSw10 and BSw4 are fed by diffuse flow (Oster et al. 2021).

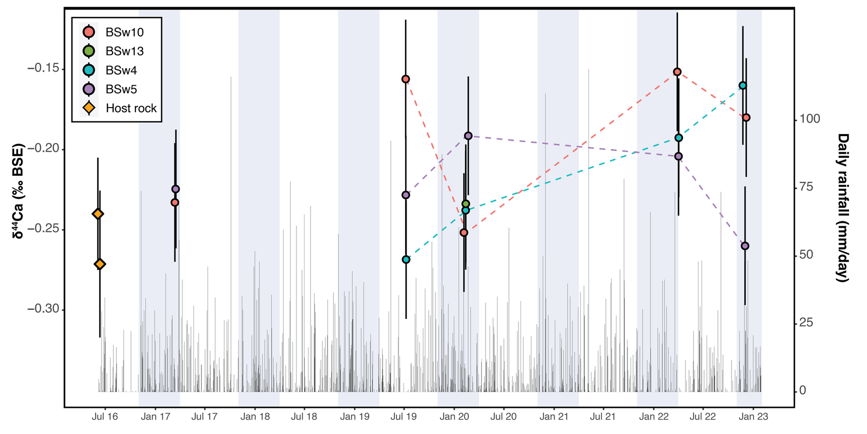

Figure 9. BS drip water δ^{44}Ca data with daily rainfall amounts from Cookeville, TN. Gray bars and symbols same as Fig. 5.

Discussion

- We calculate the fraction of calcium remaining in solution (f) for drip waters and modern calcite using Eq. 1 using a cave-specific fractionation factor ($\alpha_{calcite/water}$) and assuming the host rock to be the δ^{44}Ca source for infiltrating waters.

- Drip water and modern calcite f values range from 0.5, representing removal of ~50% of Ca originally dissolved in the karst water via PCP, to >1, representing no Ca removal via PCP (Fig. 10).

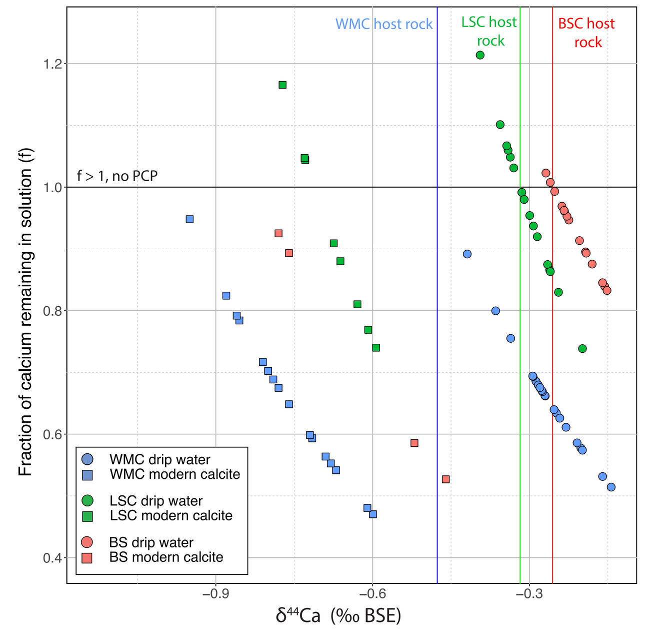

Figure 10. δ^{44}Ca and calculated f value for WMC, LSC, and BS drip waters and modern calcite. Drip water δ^{44}Ca measurements that are more negative than the corresponding host rock value generate f values great than 1, indicating no removal of Ca via PCP during flow.

Relationship between rainfall, δ^{44}Ca, and PCP from modern calcite at WMC

- PCP reconstructions from three of four WMC sites positively correlate with rainfall rates during the monitoring period.
- This is evidence that PCP reconstructions from stalagmites can be used to reconstruct past rainfall variability
- More modern calibration work will help better constrain cave-specific relationships between rainfall, δ^{44}Ca, and PCP

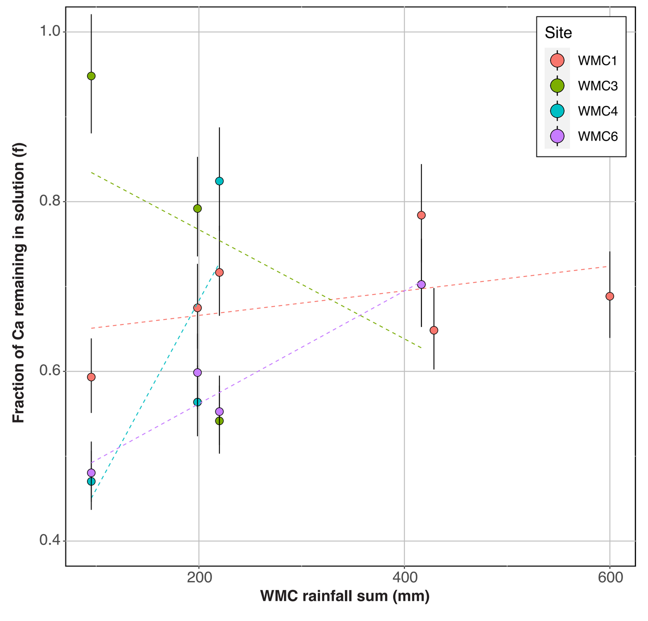

Figure 11. WMC modern calcite δ^{44}Ca values and daily rainfall rates. Points show the time span of calicte formation. Gray bars same as Fig. 5.

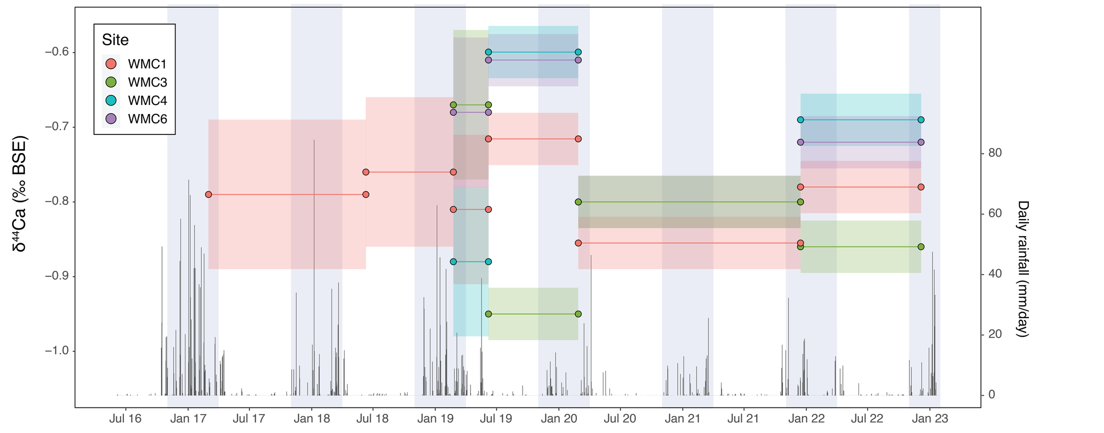

Figure 12. WMC modern calcite f values vs. the amount of rain that fell during the interval when the formed.

Influence of flow path length

- Deeper WMC sites exhibit lower f values, higher Ba/Ca relative to shallower sites, indicating more PCP occuring with depth.
- At WMC, δ^{44}Ca covaries with trace element ratios, perhaps indicating shared PCP control

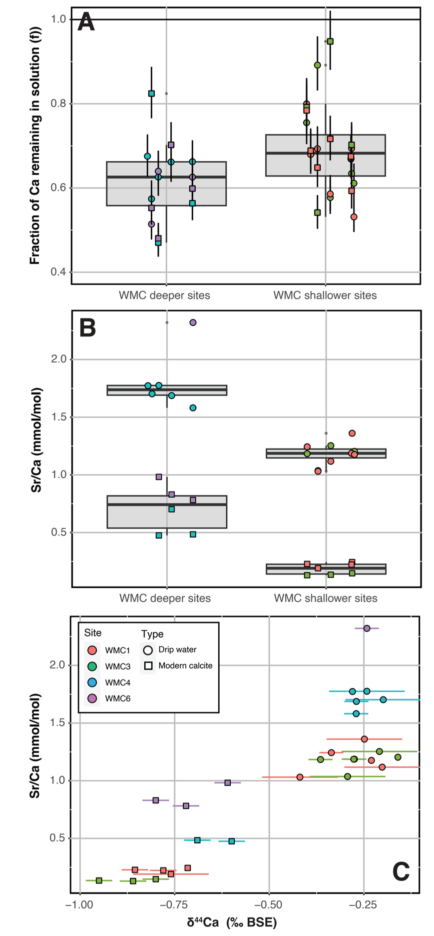

Figure 12. WMC water and modern calcite f values (A) and Sr/Ca data (B) from deeper (WMC4, 6) and shallower (WMC1, 3) sites. Sr/Ca vs. δ^{44}Ca (C). Spearman's rho is 0.6 for drip waters (p=0.03) and 0.7 for calcite (p=0.02).

Diffuse flow:

- Less variability in drip rate, consistent year-round
- Wider range of f values, more PCP

vs.

Fracture flow:

- Highly variable drip rate, seasonally dry
- Tighter range of f values, less opportunity for PCP

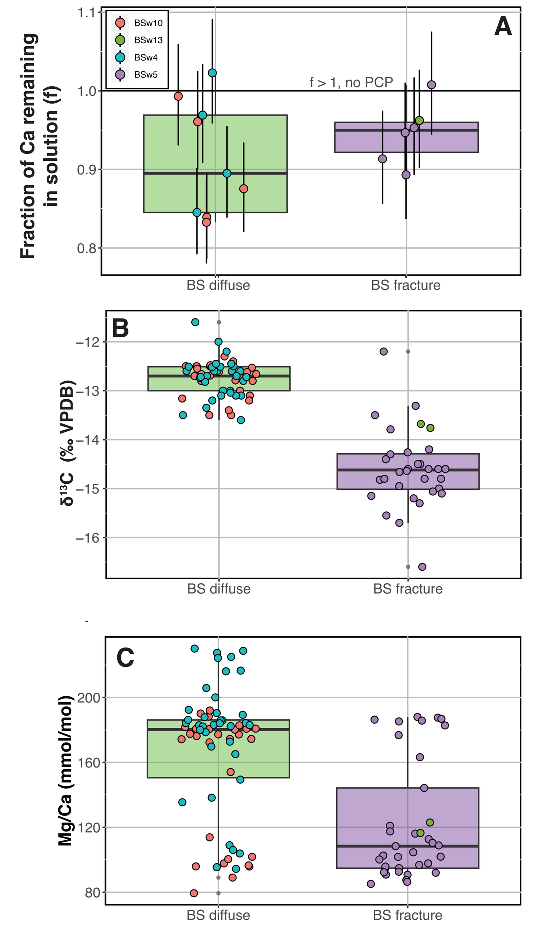

Figure 13. BS water f values (A), δ^{13}C data (B), and Mg/Ca data from diffuse flow (BSw4, 10) and fracture flow (BSw5, 13) sites.

Evidence of seasonal infiltration?

- Summer LSC drip waters tend to display lower f values, higher δ^{13}C and Mg/Ca, consistent with drier summer conditions allowing for more PCP.
- A seasonal signal is not evident at WMC.

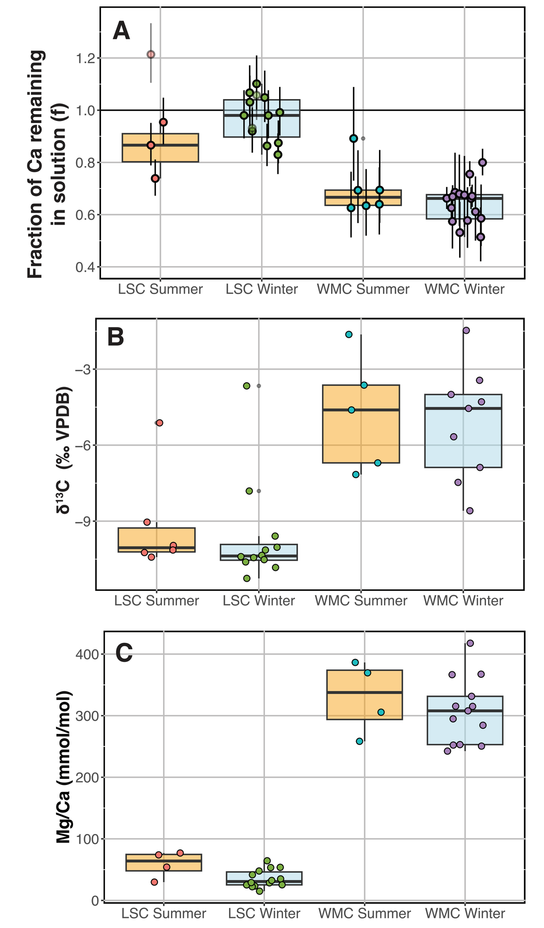

Figure 14. LSC and WMC water f values (A), δ^{13}C data (B), and Mg/Ca data from drip waters collected during the arid summer vs. the wet winter.

Citations

[1] Owen, R. A., Day, C. C., Hu, C. Y., Liu, Y. H., Pointing, M. D., Blättler, C. L., & Henderson, G. M. (2016). Calcium isotopes in caves as a proxy for aridity: Modern calibration and application to the 8.2 kyr event. Earth and Planetary Science Letters, 443, 129–138.

[2] Reynard, L. M., Day, C. C., & Henderson, G. M. (2011). Large fractionation of calcium isotopes during cave-analogue calcium carbonate growth. Geochimica et Cosmochimica Acta, 75, 3726–3740.

[3] Lechleitner, F. A., Day, C. C., Kost, O., Wilhelm, M., Haghipour, N., Henderson, G. M., & Stoll, H. M. (2021). Stalagmite carbon isotopes suggest deglacial increase in soil respiration in western Europe driven by temperature change. Clim. Past, 17(5), 1903–1918.

[4] Li, X., Cui, X., He, D., Liao, J., & Hu, C. (2018). Evaluation of the Heshang Cave stalagmite calcium isotope composition as a paleohydrologic proxy by comparison with the instrumental precipitation record. Scientific Reports, 8, 2615.

[5] de Wet, C. B., Erhardt, A. M., Sharp, W. D., Marks, N. E., Bradbury, H. J., Turchyn, A. V., et al. (2021). Semiquantitative estimates of rainfall variability during the 8.2 kyr event in California using speleothem calcium isotope ratios. Geophysical Research Letters, 48, e2020GL089154.

[6] Giesche, A., Hodell, D.A., Petrie, C.A. et al. Recurring summer and winter droughts from 4.2-3.97 thousand years ago in north India. Commun Earth Environ 4, 103 (2023).

Acknowledgments

This work is funded by the following grants:

- The Geological Society of America Gradtuate Student Research Grant
- The Karst Waters Institute Wilson Scholarship
- The Cave Research Foundation Philip M. Smith Graduate Student Research Grant
- The National Speleological Society Ralph W. Stone Research Fellowship